INVESTIGATION OF THE CRUSTAL STRUCTURE IN THE MIDDLE EAST FROM BODY-WAVE ANALYSIS

Roland Gritto[1], Matthew S. Sibol[1], Pierre Caron[1], Hafidh A. Ghalib[1], Bakir S. Ali[2], and Ali A. Ali[3]

Array Information Technology[1], Sulaimaniyah Seismological Observatory[2], and
Baghdad Seismological Observatory[3]

Sponsored by the Air Force Research Laboratory

Award No. FA8718-10-C-0003
Proposal No. BAA09-04

ABSTRACT

We present results of crustal studies obtained with seismic waveform data from the Northern Iraq Seismic Network (NISN), the Iraq Seismic Network (ISN), the North Iraq Seismic Array (KSIRS), the Iranian National Seismic Network (INSN), and the Iran Seismic Telemetry Network (ISTN). With the exception of ISTN, all of these networks operate modern broadband seismic stations. These data will be supplemented by waveforms from the Eastern Turkey Seismic Experiment (ETSE) as well as by bulletin data from Kandilli Observatory and Earthquake Research Institute (KOERI) and International Seismological Centre (ISC) stations throughout the Middle East. This effort generates an unprecedented dataset for this region consisting of 173 seismic stations, including 53 high-quality broadband stations and over 58,000 local and regional events. The data offer maximum coverage throughout the region to conduct double-difference tomography generating high-resolution (¼–½ degree) 3D P- and S-wave velocity models of the crust. We adopt a joint-inversion approach that solves simultaneously for hypocenter locations and velocity estimates. The high-resolution velocity models will cover an area from central Turkey to the eastern border of Iran and thus help to better identify and more precisely locate future events in this region. The Zagros Mountains exhibit tectonic features resulting from the collision of the Arabian and Eurasian plates. Our investigations of Pn and Pg anisotropy throughout the Zagros Mountains in northern Iraq reveal azimuthal velocity variations on the order of 2%.

OBJECTIVES

This study is a major endeavor to construct 3D velocity models of the Earth's crust in the Middle East by integrating the highest-quality seismic datasets currently available from local and regional seismic networks. The comprehensive seismic dataset will include high-quality waveform data from the INSN, ISTN, NISN, ISN, KSIRS and ETSE. These waveform data will be supplemented by bulletin data from KOERI for stations in Turkey and the International Seismological Centre (ISC) for stations throughout the Middle East. NISN has operated ten broadband stations in northeastern Iraq since late 2005 and was supplemented by the five-element broadband KSIRS in 2007. In the past two years, the former ISN was reestablished with the deployment of six broadband stations throughout Iraq. The objectives of the current project include the development of high-resolution crustal and upper mantle velocity models of the Middle East, including central and western Turkey, Iraq, and Iran. The results of this study will provide important information for future studies in the form of a GT5 database, high-resolution 3D P- and S-wave velocity models, and improved hypocenter relocations.

RESEARCH ACCOMPLISHED

Waveform Analysis of Iraqi NISN Waveform Data

The goal of this analysis is to obtain accurate travel times for local and regional body wave phases including P, Pn, Pg, S, Sn, and Lg waves. These phase arrivals and the associated hypocenter locations will subsequently form a bulletin that will be the input for 3D P- and S-wave velocity tomography throughout the Middle East.

Towards this goal, we have analyzed waveform data recoded by NISN from January 2006 to December 2008. The NISN waveform data were supplemented by Iranian broadband (INSN) and short period (ISTN) recordings to improve the accuracy of hypocenter locations. The waveform data were first analyzed using an automatic event detector module of Antelope to obtain preliminary phase detections. The detections were subsequently quality controlled by AIT staff and, if necessary, phase arrivals were corrected by hand. Once the quality of the arrivals was assured, hypocenter locations were calculated based on a 1D six-layer velocity model obtained for the Zagros Fold and Thrust Zone by Pasyanos et al. (2004). Once hypocenter locations were determined, travel-time distance curves were obtained to appraise the quality of phase picks and to reveal systemic errors that may have been present in the analysis.

The complete set of travel-time curves with quality-controlled phase arrival picks of all NISN waveform data from 2006 to 2008 is presented in Figure 1. The respective 1D velocity estimates as given are with uncertainties of one standard deviation. The low standard deviation of 0.5% or less is due to the high level of quality control applied to the data. The database of NISN, INSN, and ISTN travel-time picks comprises over 3,500 events, including 15,100 Pg arrivals, 11,900 Pn arrivals, 16,200 Sg/LG arrivals, and 5,800 Sn arrivals.

The P- and S-wave ray coverage associated with these phase picks are presented, respectively, in Figures 2 and 3. It can be seen that for both P- and S-waves, the distribution of seismicity is concentrated along the Zagros Mountains from northeastern Iraq to Bandar Abbas in southern Iran. Accordingly, the ray coverage is densest in this region, while gaps are apparent in eastern Iran, western Iraq, and Syria. It is noted that eastern Turkey will be covered by seismic data collected during the ETSE campaign and by data obtained from the KOERI network in Turkey (see below). Additionally, these NISN data are currently supplemented by waveform records obtained from ISTN in eastern and southern Iran, and ISC travel-time data throughout the whole region are summarized in the following section.

Waveform Analysis of Iranian ISTN Waveform Data

We have supplemented the NISN data with waveforms recorded by the ISTN to improve ray density in eastern and southern Iran. Particular attention is given to those events not covered by the NISN analysis described above. The waveform data, which cover the time period from January 2006 to December 2008, contain preliminary phase picks determined by Iranian Seismological Center (IRSC) staff. Our recent efforts are concerned with ensuring quality control and correcting phase picks, as well as determining phase arrivals that may have been missed by IRSC staff.

The objective of this task is to increase ray coverage in eastern and southern Iran to improve resolution of the tomographic imaging for crustal structure in the region. During this task we concentrate on events with a high number of reported phase picks to optimize ray coverage. Preliminary results of processed data from early 2007

yielded 75 events with 309 Pg phase arrivals, 311 Pn phase arrivals, 356 Lg phase arrivals, and 73 Sn phase arrivals. The associated ray coverage is presented in Figures 4 and 5. The figures display the ISTN network (red triangles), the NISN network (gray triangles), the 75 analyzed events (green circles), the Pg- and Pn-wave ray coverage (Figure 4, blue lines), and Lg- and Sn-wave ray coverage (Figure 5, red lines). The objective of increasing ray coverage in eastern and southern Iran is already emerging in the figures. It can be seen that the 75 selected events have primarily been recorded by the eastern sub-networks of ISTN increasing the ray coverage in this region of Iran. We will continue to analyze ISTN waveform data for the whole period from 2006 to 2008.

International Seismological Centre (ISC) Bulletin Data

Bulletin data from ISC stations in the Middle East were obtained for a period from 2000 to 2008 to increase data coverage in regions where the NISN, KSIRS, ISN, INSN, ISTN, and ETSE networks have limited or no detection capabilities. The ISC bulletin data, obtained for a rectangular area between 30^{o} and 64^{o} eastern longitude and 22^{o} and 46^{o} northern latitude, are composed of 23,500 events. The distribution of ISC stations and seismicity within this region is presented in Figure 6. It can be seen how the distribution complements the region covered by the aforementioned networks particularly in eastern Turkey, the rift zones of the Dead Sea and Red Sea, and northern Iran. The associated ray coverage (not shown here) should improve the resolution of velocity estimates in the western part of the region under investigation.

The ISC bulletin produced 54,500 Pg, 157,000 Pn, 40,200 Sg/Lg, and 36,100 Sn phase arrivals. We refined quality control of the data and eliminated poor quality picks using only those events that have a minimum of 10 defining phases and a root mean square residual of less than 2 seconds. A subset of the refined ISC phase picks from January 2006 through July 2008 can be seen in Figure 7. The quality of the data is apparent, with only a few phase picks with lesser quality remaining. These picks will be eliminated during the inversion process. Furthermore, it can be seen that the maximum hypocentral distance of Pn and Sn phases extends to 2,250 km, which is considerably longer than, for example, for the, NISN phase picks presented in Figure 1. Therefore, the ISC bulletin will provide supplemental data that extends the range of the tomographic analysis to a larger region.

Eastern Turkey Seismic Experiment (ETSE)

The ETSE, conducted from 1999 to 2001 across the East Anatolian Plateau and the northernmost Arabian plate was designed to improve the understanding of the Bitlis suture zone and of the crustal dynamics of the East Anatolian block (Sandvol et al., 2003). The experiment consisted of a 29-station temporary broadband PASSCAL network operated for 21 months from October 1999 to August 2001. Data recording was done with a sample rate of 40 sps. The network was shaped in a triangular pattern covering most of eastern Turkey, with an average station separation of approximately 50 km. The seismicity in this region was about 10 events per day, with a total of 1,165 earthquakes located during the time span of the deployment. The ETSE network and seismicity recorded during deployment are presented in Figure 8.

The earthquakes were categorized based on the quality of their locations, with 792 events falling in the best class with a location error of less than 5 km. Although the region exhibits a high degree of attenuation, the recorded waveforms were generally of good quality with Pg, Pn, Sg/Lg, and Sn phases apparent on the seismograms. All of the listed events are concentrated above 30 km depth as no sub-crustal events were recorded beneath the Anatolian Plateau during the experiment. The lack of deeper seismicity is attributed to the absence of mantle lithosphere caused by the break-off of the northward subducting slab, which brings the lower crust in direct contact with hot asthenosphere, a likely cause for volcanism throughout the Anatolian Plateau. The ETSE experiment produced high-quality waveform data that are complementary to the KOERI and ISC data obtained for eastern Turkey. We expect the resolution and accuracy of our tomography results to benefit from the inclusion of the ETSE waveform data.

Kandilli Observatory and Earthquake Research Institute (KOERI) Bulletin Data

The KOER) operates a network of 76 seismic stations throughout Turkey. In 1997 the first digital broadband station was installed at Kandilli, followed in 1998 by the installation of a five-station digital radio-telemetered network encompassing the Marmara Sea. Full-scale conversion to digital recording began within KOERI after the August 17, 1999, Mw 7.4 Izmit earthquake. At present, the network operates 57 short-period, 14 broadband, and 5 semi-broadband stations. The locations of the stations are presented in Figure 9. For the current project, we will supplement our waveform data with all available bulletin data from the KOERI network. Because the waveform data collected by ETSE (1999–2001) are not concurrent with the waveform data currently recorded by NISN, ISN, KSIRS, INSN, and ISTN, the addition of KOERI data will help to improve resolution in the western part of our

study area by providing parametric data from events that may have been simultaneously recorded by the other networks. The complete KOERI catalogue, which we obtained from Kandilli Observatory for the period of 1900 to 2009, contained 130,571 earthquake including epicentral information, depth, and magnitude.

Azimuthal P-Wave Velocity Variations in the Zagros Fold and Trust Zone

While crustal anisotropy may be indicative of tectonic stresses and alignments of faults and fracture zones, upper mantle anisotropy may indicate flow or stress pattern in the lithosphere in response to tectonic loading in the region. To develop an understanding of azimuthal variations of the velocity structure in the crust and upper mantle in the Zagros Fold and Thrust Zone, we examined a set of 9,000 crustal Pg phase arrivals and 5,000 refracted Pn phase arrivals from waveforms recorded by NISN.

The results of the anisotropy analysis are presented in Figures 10 and 11. Figure 10 shows the Pg-wave velocity values as a function of azimuth. The azimuth in this case is the angle between the epicenters and the center of the NISN network. Each point on the diagram represents one phase pick of a Pg arrival. The distribution of measurements reflects the distribution of seismicity in the region relative to the location of the NISN network. The high rate of seismicity along the Zagros zone is represented by the large number of measurements between 110^o and 140^o azimuth. Similarly, the seismicity throughout the Taurus Mountains and eastern Turkey is represented by the increase in measurements between 280^o and 310^o azimuth. In contrast, the relatively aseismic Arabian plate is represented by the paucity of measurements between 210^o and 240^o azimuth.

In order to appraise the degree of anisotropy, the velocity variation along the radial axis of the diagram needs to be evaluated. Considering the average Pg-wave velocity of 5.97 km/s for this region, a change of 0.25 km/s represents ~ 4% variation in velocity. It can be seen in Figure 10 that for the northeastern quadrant, between 0^o and 90^o azimuth, the average Pg velocity is about 3% lower than average. This reduction in velocity may be explained by the strike of the Zagros zone, which separates the NISN network from the source of seismicity in northern Iran. Crustal P-waves originating in this region need to propagate across the strike of the Zagros zone to reach the network. It is likely that the interaction with the faults in the Zagros reduces the average velocity to the observed values. In contrast, the average velocities for the southeast and northwest quadrants are relatively close to the average of 5.97 km/s, indicating that the propagation associated with these ray paths is predominantly parallel to the strike of the Zagros zone and therefore not slowed down. The results for the southwest quadrant cannot be cleanly categorized due to the lack of phase picks, which is evident by the larger standard deviations for the velocity estimates. We expect that a clearer pattern will emerge with the addition of phase picks related to seismicity in the Arabian Peninsula.

The results for the Pn-wave velocities are presented in Figure 11 and are similar to those shown in Figure 10. The average Pn-wave velocity for the region is 8.25 km/s, which yields a 3% velocity change for each 0.25 km/s deviation from the average. With this calibration in mind, the interpretation of the data in Figure 11 yields similar results compared to those in Figure 10. However, the magnitude of velocity reduction associated with wave propagation from the northeast appears reduced relative to the case of crustal phases. For the Pn waves, velocity reductions of 1%–2 % are observed for most phases from this region. Results for the southeast quadrant suggest a 1.5%–2.5% increase in speed relative to the average velocity, indicating a possible propagation path aligned with upper mantle flow patterns that may be the result of tectonic features in the crust. However, in contrast to results in Figure 10, velocity estimates from the northwest quadrant are slightly lower than average for Pn waves in the upper mantle. For the southwest quadrant, the results are again inconclusive owing to the lack of phase picks from this region.

To substantiate the findings in Figures 10 and 11, the actual phase count for Pg, Pn, Sg, and Sn phases is investigated, to ascertain whether possible blockage in the crust or upper mantle may indicate structural features or elevated temperatures, respectively. However, because the number of observed phases is also a function of the number of observed earthquakes, the phase count for each phase was normalized by the number of earthquakes. The results are presented in Figure 12, where the normalized phase count for Pg, Pn, Sg, and Sn phases are given in panels a, b, c and d, respectively. The phase count diagram for Pg, reveals a relatively large lobe in the southwesterly direction, indicating the location of events with relatively uninhibited wave propagate towards NISN. In contrast, the low counts in the northwesterly and southeasterly directions may indicate structural blockage of the Pg phases within the crust. However, this obstruction may be somewhat localized as the velocity of the phases that are observed at NISN is not reduced relative to the average (see Figure 10). Combining the results of Figure 12a with 12b, it may be concluded that in the southeasterly direction, the blockage might be restricted to the crust

because Pn phases propagating in the upper mantle reach NISN in greater numbers. Conversely, the low number of observed Pn phases from the northwesterly direction could be an indication of an increase in lower crust or upper mantle temperatures in Eastern Turkey, which would support findings by Al-Lazki et al. (2004) and Gök et al. (2003).

The results of S-wave phase counts, in Figure 12c and 12d, support the interpretation give for the P-wave observations above. The spatial distribution of the Sg-wave phases (Figure 12c) correlates highly with that of the Pg phases, even though the number of Sg phases is slightly higher. The Sn phase count in the southeasterly direction (Figure 12d) is similar to that of the Pn phases, which supports the interpretation that the upper mantle is relatively free of blockage for refracted phase in that direction. In contrast, the Sn phase count in northwesterly directions is very low, which supports the interpretation of an increase in lower crust and/or upper mantle temperatures in Eastern Turkey as mentioned above.

The presented analysis would benefit from the investigation of S-wave anisotropy in the upper mantle. S-wave splitting due to anisotropy generates two polarized waves that propagate with different velocities and can be observed on rotated horizontal and vertical components. However, rotating the components and re-picking Sn phase arrivals is beyond the scope of the current study.

CONCLUSIONS AND RECOMMENDATIONS

The objectives of the current project include the development of high-resolution crustal and upper mantle velocity models of the Middle East, including central and western Turkey, Iraq, and Iran. Towards this goal we have compiled a comprehensive database that includes waveform data from the NISN, ISN, KSIRS, INSN, and ISTN, supplemented by bulletin data from KOERI and the ISC. The database will be the basis for double-difference tomography generating high-resolution (¼–½ degree) 3D P- and S-wave velocity models of the crust.

Analysis of anisotropic variation of the P-wave velocities in the crust and upper mantle of the Zagros Fold and Thrust Zone reveals results that may indicate the presence of tectonic features resulting from the collision of the Arabian and Eurasian plates. The anisotropy results in combination with phase counts of P- and S-wave arrivals point toward higher temperature in the lower crust and upper mantle in eastern Turkey and the Bitlis suture zone.

The results of this study will provide important information for future studies in the form of a GT5 database, high-resolution 3D P- and S-wave velocity models, and improved hypocenter relocations.

REFERENCES

Al-Lazki A. I., E. Sandvol, D. Seber, M. Barazangi, N. Türkelli, and R. Mohamad (2004). Pn tomography imaging of the mantle lid velocity and anisotropy at the junction of the Arabian, Eurasian and African plates, *Geophys. J. Int.* 158: 1024–1040.

Gök, R., E. Sandvol, N. Türkelli, D. Seber, and M Barazangi (2003), Sn attenuation in the Anatolian and Iranian plateau and surrounding regions, *Geophys. Res. Lett.*, 30:24, 8042, doi:10.1029/2003GL018020.

Pasyanos, M. E., W. R. Walter, M. P. Flanagan, P. Goldstein, and J. Bhattacharyya (2004). Building and testing an a priori geophysical model for western Eurasia and North Africa, *Pure Appl. Geophys.* 161: 235–281, 0033 – 4553/04/020235 – 47, DOI 10.1007/s00024-003-2438-5.

Sandvol, E., N. Türkelli, and M. Barazangi (2003). The eastern Turkey seismic experiment: The study of a young continent-continent collision, *Geophys. Res. Lett.* 30: 24, 8038, doi:10.1029/2003GL018912.

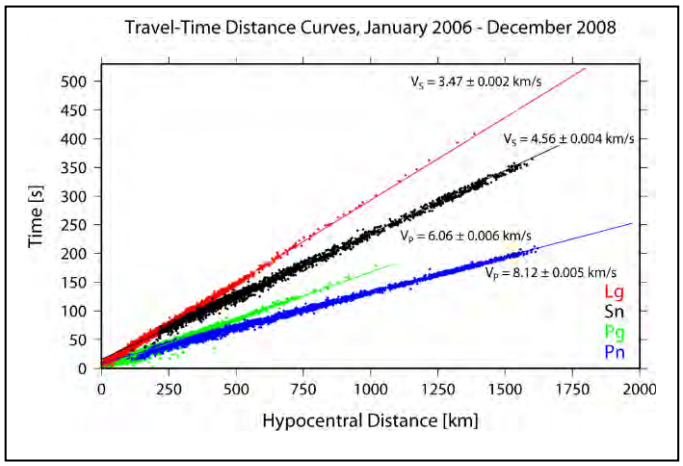

Figure 1. Travel-time distance curve for phase picks obtained from NISN, INSN, and ISTN waveform data from January 2006 through December 2008.

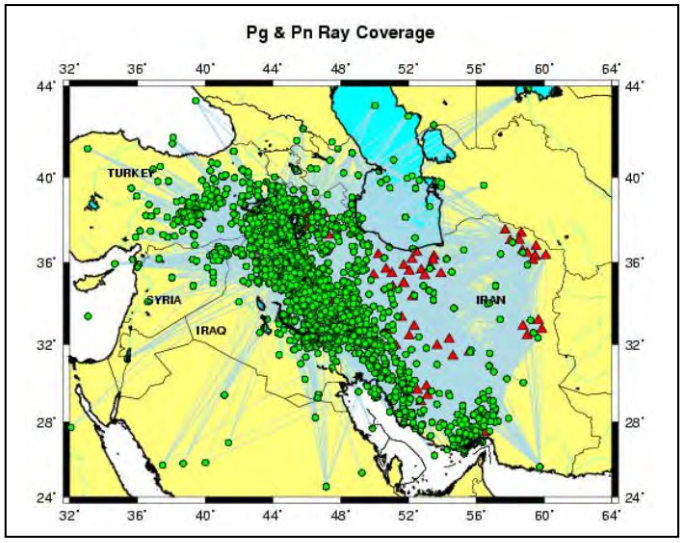

Figure 2. Distribution of Middle Eastern seismicity from January 2006 through December 2008, as recorded by NISN, INSN, and ISTN. The green dots represent epicenter locations, the partly covered red triangles indicate the station distribution of the three networks, and the blue lines are the ray paths associated with Pg- and Pn-wave phase picks determined from the waveform data.

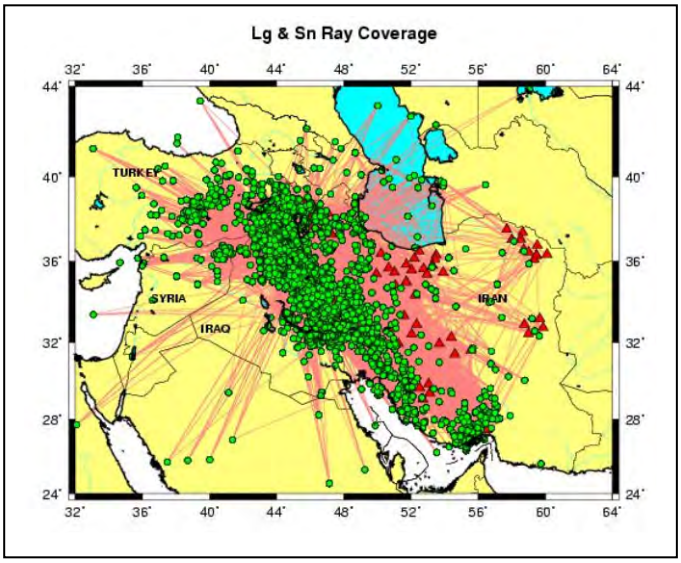

Figure 3. Same as Figure 2 for Sg/Lg- and Sn-wave phase picks.

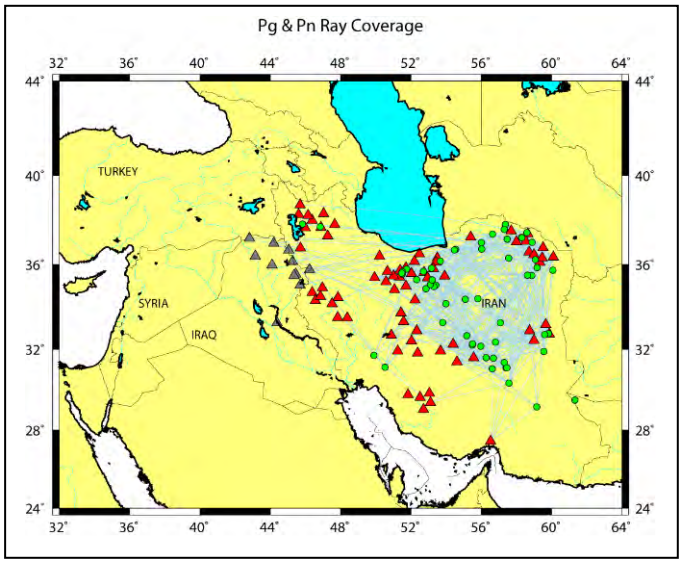

Figure 4. Distribution of seismicity in eastern Iran recorded in early 2007 by ISTN. The green dots represent epicenter locations, the red and gray triangles denote the location of the ISTN and NISN networks (respectively), and the blue lines are the ray paths associated with Pg- and Pn-wave phase picks determined from the waveform data.

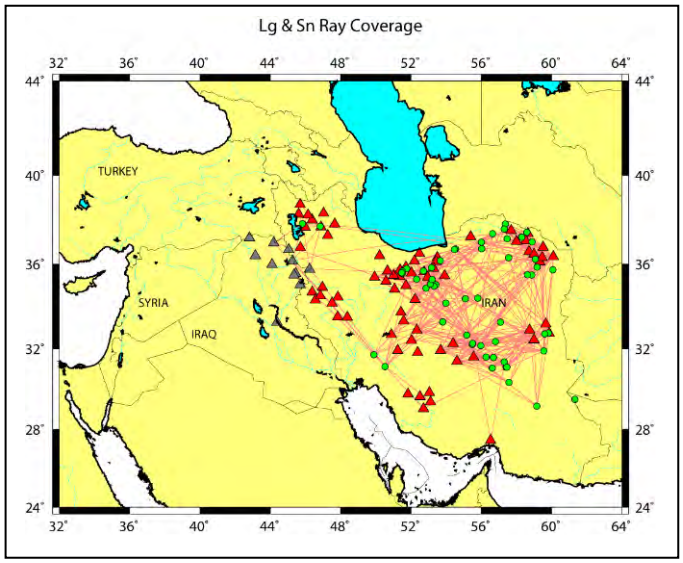

Figure 5. Same as Figure 4 for Lg- and Sn-wave phase picks.

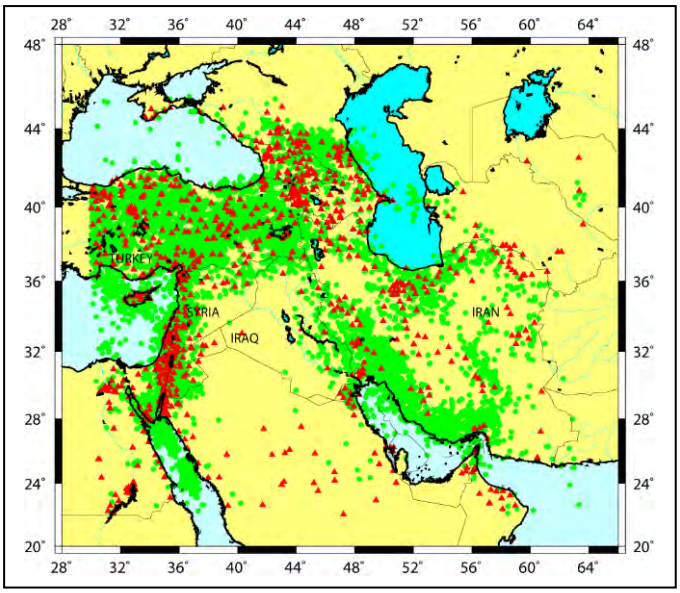

Figure 6. Distribution of ISC stations and recorded seismicity from January 2000 through July 2008. The red triangles and green dots represent ISC stations and earthquakes, respectively, within a rectangle area between 30° and 64° eastern longitude and 22° and 46° northern latitude.

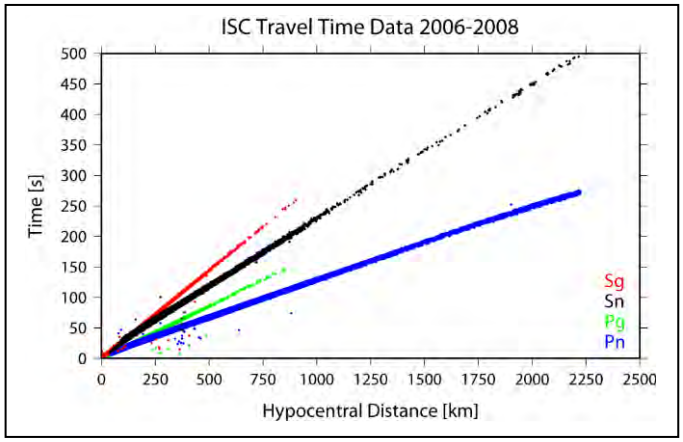

Figure 7. Travel-time distance curves for high-quality P- and S-wave phase picks, as reported by ISC from January 2006 through July 2008.

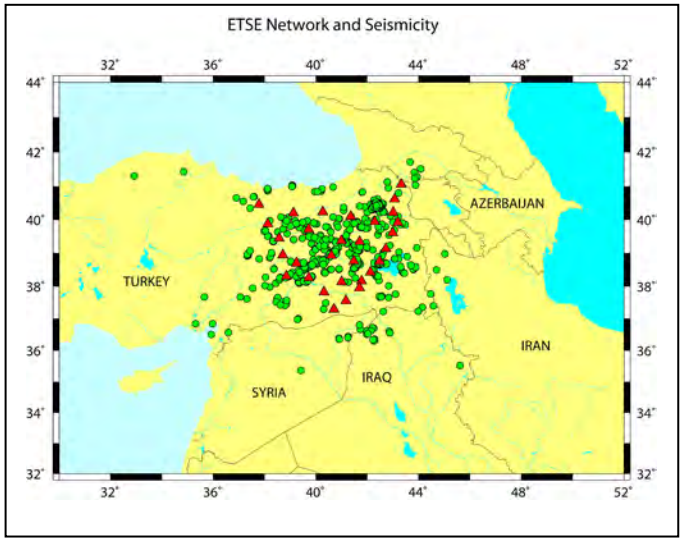

Figure 8. Map indicating the location of the ETSE network (red triangles) and seismicity (green circles) recorded during the deployment period. A total of 1,165 earthquakes were recorded and located with the network.

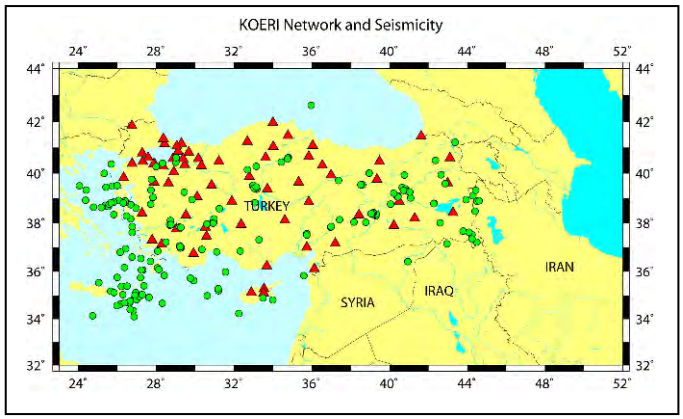

Figure 9. Location of the KOERI network (red triangles) and distribution of seismicity $M_L \geq 4.0$ from April 2006 to April 2008 (green circles).

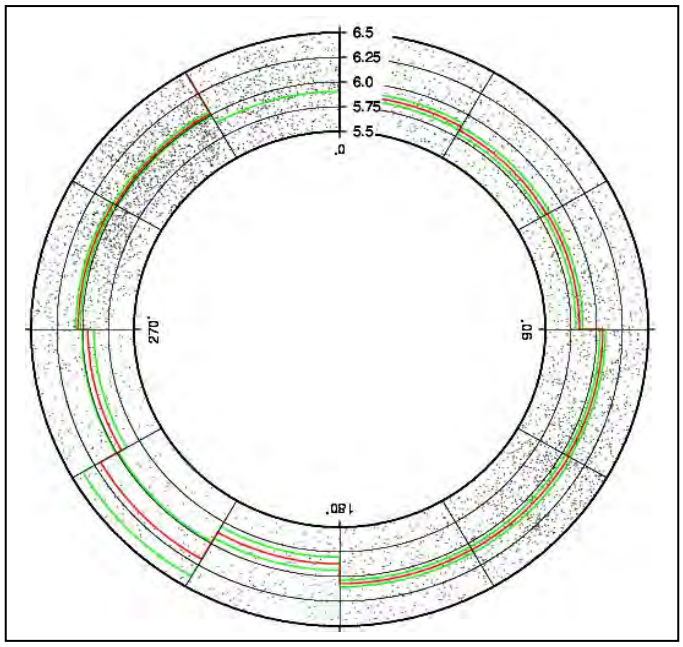

Figure 10. Azimuthal distribution of Pg velocity centered at the midpoint of NISN. The radial values denote Pg velocity values from 5.5 km/s to 6.5 km/s while the azimuthal values denote geographic directions from north, to east, to south and west, indicated by 0^o, 90^o, 180^o, 270^o, respectively. The black dots represent velocity estimates for each phase pick derived from NISN waveform data from January 2006 through March 2008. The red lines are mean velocity values averaged over 30^o intervals, while the red lines denote one standard deviation from the mean. The average Pg-wave velocity is 5.97 km/s for the northern Zagros region.

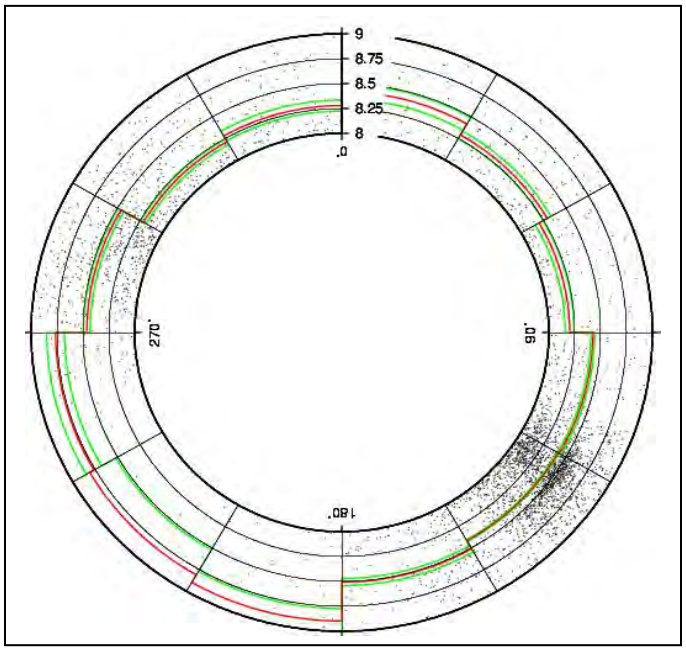

Figure 11. Same as Figure 10 for Pn velocity. The radial values denote Pn velocity values from 8 km/s to 9 km/s. The average Pn-wave velocity is 8.25 km/s for the northern Zagros region.

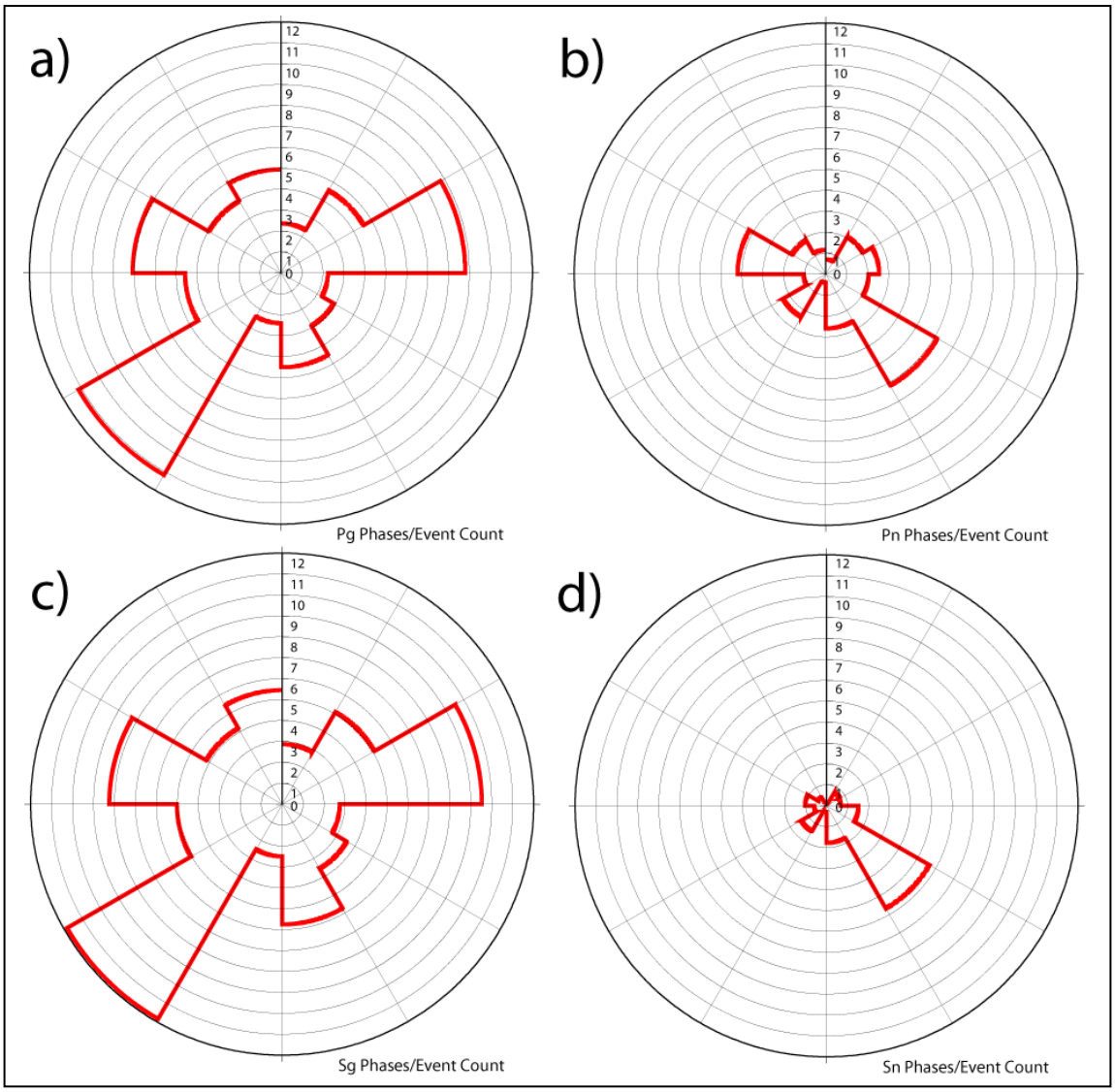

Figure 12. Azimuthal distribution of the number of observed phases normalized by the number of observed earthquakes for NISN waveform data from January 2006 through March 2008. The red lines denote normalized phase counts averaged over 30° intervals: (a) Pg phase count, (b) Pn phase count, (c) Sg phase count, and (d) Sn phase count.